

# A time-dependent jet model for the emission from Sagittarius A\*

Dipankar Maitra<sup>1</sup>, Sera Markoff<sup>1</sup>, and Heino Falcke<sup>2,3</sup>

<sup>1</sup> Astronomical Institute “Anton Pannekoek”, University of Amsterdam, Science Park 904, 1098 XH Amsterdam, The Netherlands

<sup>2</sup> Department of Astrophysics, Institute for Mathematics, Astrophysics and Particle Physics, Radboud University, P.O. Box 9010, 6500 GL Nijmegen, The Netherlands

<sup>3</sup> ASTRON, Oude Hoogeveensedijk 4, 7991 PD Dwingeloo, The Netherlands

## ABSTRACT

*Context.* The source of emission from Sgr A\*, the supermassive black hole at the Galactic Center, is still unknown. Flares and data from multiwavelength campaigns provide important clues about the nature of Sgr A\* itself.

*Aims.* Here we attempt to constrain the physical origin of the broadband emission and the radio flares from Sgr A\*.

*Methods.* We developed a time-dependent jet model, which for the first time allows one to compare the model predictions with flare data from Sgr A\*. Taking into account relevant cooling mechanisms, we calculate the frequency-dependent time lags and photosphere size expected in the jet model. The predicted lags and sizes are then compared with recent observations.

*Results.* Both the observed time lags and size-frequency relationships are reproduced well by the model. The combined timing and structural information strongly constrain the speed of the outflow to be mildly relativistic, and the radio flares are likely to be caused by a transient increase in the matter channelled into the jets. The model also predicts light curves and structural information at other wavelengths which could be tested by observations in the near future.

*Conclusions.* We show that a time-dependent relativistic jet model can successfully reproduce: (1) the quiescent broadband spectral energy distribution of Sgr A\*, (2) the observed 22 and 43 GHz light curve morphologies and time lags, and (3) the frequency-size relationship. The results suggest that the observed emission at radio frequencies from Sgr A\* is most easily explained by a stratified, optically thick, mildly relativistic jet outflow. Frequency-dependent measurements of time-lags and intrinsic source size provide strong constraints on the bulk motion of the jet plasma.

**Key words.** galaxies: jets — galaxies: active — galaxies: nuclei — black hole physics — Galaxy: center — radiation mechanisms: general

## 1. Introduction

The compact radio source Sagittarius A\* (hereafter Sgr A\*), at an estimated distance of  $8.4 \pm 0.6$  kpc (Reid et al. 2009) and mass of  $\sim 4 \times 10^6 M_{\odot}$  (Ghez et al. 2008; Gillessen et al. 2009), is our closest supermassive black hole. When compared to other active galactic nuclei (AGN), Sgr A\* is extremely under-luminous at all wavelengths, suggesting either that the mass accretion rate ( $\dot{M}$ ) onto the black hole, or the radiative efficiency, is very low. Polarization measurements suggest that  $\dot{M} \leq 10^{-7} M_{\odot}/\text{yr}$  (Marrone et al. 2007). Recent multiwavelength campaigns that have monitored Sgr A\* simultaneously from radio to X-rays have found that even though the luminosity of Sgr A\* is low relative to its AGN counterparts, its emission is quite variable at all wavelengths. Flaring activity at both sub-mm and higher frequencies has been observed on timescales ranging from minutes to hours, suggesting that the emission at these frequencies is produced very close to the supermassive black hole, probably within a few tens of gravitational radii ( $R_g = GM/c^2$ ). Although flaring appears to be nearly simultaneous at these frequencies (Marrone et al. 2008; Eckart et al. 2008; Dodds-Eden et al. 2009), the flares seem to have an increasingly long time-delay at longer wavelengths. For example, Yusef-Zadeh et al. (2008) found that the 43 GHz flares precede the 22 GHz flares by  $20 \pm 10$  minutes, and that 350 GHz flares precede those of 43 GHz by 30 – 60 minutes.

The physical origin of the observed electromagnetic radiation from Sgr A\* has been under active debate for more than a decade. Attempts to model the emission from Sgr A\* can be broadly classified into two categories: (1) accretion inflow models (Melia 1992; Narayan et al. 1998; Liu & Melia 2002; Yuan et al. 2006), and (2) relativistic outflow/jet models (Falcke & Biermann 1999; Falcke & Markoff 2000; Yuan et al. 2002). The radio, NIR, and X-ray flare light curves were modeled assuming expansion of a spherical plasma blob (see e.g., Yusef-Zadeh et al. 2008; Eckart et al. 2009). Recently Falcke et al. (2009) suggested that the radio time-lag data and measurements of intrinsic size at various frequencies (e.g., Bower et al. 2004; Shen et al. 2005; Doeleman et al. 2008) can be used to resolve the degeneracy between inflow and outflow models. It has long been suspected that radio flares such as those reported by Yusef-Zadeh et al. (2008) could be “smoking gun evidence” of jets in sources such as Sgr A\* (Falcke 1999b).

While jets have not been directly imaged in Sgr A\*, several observations strongly suggest the presence of jets in this source. The flat/slightly inverted radio spectral energy distribution (SED) (signature of a compact self-absorbed jet in the radio; see e.g., Blandford & Königl 1979) observed from Sgr A\* are similar to those of other low-luminosity AGNs. M81 and Sgr A\* have very similar spectra and polarization properties in the cm-radio band, and M81 has been found to have weak jets (Nagar et al. 2005). Radio observations of the stellar X-ray binary system A0620–00 (Gallo et al. 2006) at almost near quiescent luminosity suggest that compact jets are present at bolometric luminosities as low as  $\sim 10^{-7} L_{\text{Edd}}$ . If jet physics and

accretion flow scale with the mass of the black hole, then Sgr A\* ( $L_{\text{bol}} \sim 10^{-9} L_{\text{Edd}}$ ) is also expected to harbor a faint, compact jet. Steady-state jet models have previously been used to model the broadband quiescent spectra of Sgr A\* successfully (Falcke & Markoff 2000; Yuan et al. 2002); steady-state models, however, cannot predict the flaring activity.

In this paper we develop a proper treatment of the time-dependent cooling processes of the particle distribution, while keeping the basic hydrodynamic outflow model the same as in Falcke (1996), allowing a semi-analytical treatment of the problem. Once dominant cooling mechanisms are taken into account, the time-dependent jet model naturally accounts for all the observational constraints, namely, (a) the broadband SED, (b) the observed light-curve morphologies and time-lags, and (c) the observed frequency–size relationship.

## 2. Model

We assume that a fraction of the accretion inflow is channelled into two symmetric, collimated supersonic outflows. The energy distribution of the radiating leptons entering the jet is assumed to be a thermal, relativistic Maxwell-Jüttner distribution. Most of the kinetic energy of the jet is assumed to be carried by cold, non-radiating baryons. The bulk speed at the base of the jet is assumed to be the sound speed, and beyond the base (or the “nozzle”) the jet plasma accelerates longitudinally via pressure gradient and expands laterally with the sound speed  $\beta_s \sim 0.4$ . We adopt the standard one-fluid approximation used in magnetohydrodynamics (MHD; see e.g. Leismann et al. 2005), and treat the magnetized jet plasma as a single-component fluid of adiabatic index 4/3. The longitudinal velocity profile is obtained by solving the relativistic Euler equation, and the magnetic field strength estimated via flux conservation (see Falcke 1996; Falcke & Markoff 2000, for details of the hydrodynamics of a pressure driven supersonic jet).

The observed spectrum from the compact jet is modeled as the sum of emission from cylindrical segments along the jet axis. Within each segment we consider the following processes influencing the local evolution of the particle distribution:

- *Synchrotron cooling*: Losses due to synchrotron emission are given by  $\dot{\gamma}_{\text{syn}} = 4c\sigma_T U_B \gamma^2 / (3m_e c^2)$ , where  $\sigma_T$  is the Thomson cross-section and  $U_B = B^2 / 8\pi$  is the magnetic energy density.
- *Inverse Compton (IC) cooling*: Losses due to IC scatterings are given by  $\dot{\gamma}_{\text{com}} = 4c \langle \sigma_{\text{KN}} U_{\text{rad}}(t) \rangle_{\gamma} \gamma^2 / (3m_e c^2)$ , where, following de Kool et al. (1989) we define  $\langle \sigma_{\text{KN}} U_{\text{rad}}(t) \rangle_{\gamma} = 4\pi/c \int \sigma_{\text{KN}}(\gamma, \nu) J_{\nu} d\nu$ . Here  $\sigma_{\text{KN}}(\nu, \gamma)$  is the Klein-Nishina correction to the scattering cross-section and  $J_{\nu}$  the mean intensity.
- *Adiabatic expansion*: Cooling due to adiabatic expansion is given by  $\dot{\gamma}_{\text{ad}} = (1/3)\gamma \nabla \cdot \mathbf{v}$ , where  $\nabla \cdot \mathbf{v}$  denotes the divergence of the bulk velocity field (Longair 1992).

For numerical discretization we assume that the plasma in each segment cools for the time it requires to cross the segment. We follow the evolution of such a “parcel” of jet plasma as it moves from one segment to another, i.e. in a comoving frame, without any particle loss/escape. For simplicity we assume that this comoving “parcel” of particles cools and radiates independently, i.e. is not influenced by its neighbors. While this is obviously a simplification, given the overall simplicity of the model

we feel this is justified. The continuity equation for the time evolution of leptons in this case is given by

$$\frac{\partial N(\gamma, t)}{\partial t} = \frac{\partial}{\partial \gamma} [\dot{\gamma}(\gamma, t) N(\gamma, t)] \quad ; \quad \dot{\gamma}(\gamma, t) = \dot{\gamma}_{\text{syn}} + \dot{\gamma}_{\text{com}} + \dot{\gamma}_{\text{ad}} \quad (1)$$

Given the low luminosity of Sgr A\* ( $\sim 10^{-9} L_{\text{Edd}}$ ), the compactness parameter ( $\ell \equiv L\sigma_T / (Rm_e c^3)$ ; see Guilbert et al. 1983) is very small ( $\ell \sim 10^{-6}$  for  $R=10 R_g$ ). Therefore pair processes are not important here. Also, there is no injection term in (1) since particle acceleration seems to be very weak or lacking in Sgr A\* (Markoff 2005). Recasting (1) as a Fokker-Planck equation, we used the fully implicit Chang-Cooper algorithm (Chang & Cooper 1970; Chiaberge & Ghisellini 1999) to solve it.

Once the time-evolved particle distribution solution is obtained, we then compute the emitted SED due to angle averaged synchrotron emission using eq.(10) of Crusius & Schlickeiser (1986) for relativistic electrons with Lorentz factor  $\geq 2$ , and using eq. (8) of Katarzyński et al. (2006) for electrons in the cyclo-synchrotron regime with Lorentz factor  $< 2$ . IC is computed incorporating the Klein-Nishina correction for scattering beyond Thomson limit following the prescription of Blumenthal & Gould (1970). The seed photons for IC are the photons produced locally by synchrotron emission (synchrotron self-Compton; SSC). In the absence of detailed spatial information of the hot stars that constitute the central star cluster close to Sgr A\* (see e.g. Genzel et al. 2000), we estimated emission from these stars by assuming 100 stars of temperature 10,000 K each, situated 0.5 parsecs from Sgr A\*. The photon density of locally produced synchrotron+SSC photons in the jet is at least 3 orders of magnitude higher than that due to total photon density from these stars, suggesting that external inverse Compton losses due to photons from the nearby cluster is not important.

Since the bulk motion of the emitting jet plasma is relativistic we first compute the Doppler factor  $\mathcal{D} = [\Gamma(1 - \beta \cos\theta)]^{-1}$ , where  $\theta$  is the angle between velocity and line of sight,  $\beta$  is the bulk speed, and  $\Gamma = 1/\sqrt{1 - \beta^2}$  is the bulk Lorentz factor. Then the observed SED is calculated by applying the appropriate special relativistic transformations of the emitted frequency and flux (see e.g. Lind & Blandford 1985), and taking into account time-lags due to the spatial extent of the flow.

For any given frequency, when the flux from each jet segment is plotted as a function of distance from the black hole, it roughly resembles a bell-shaped curve (in the self-absorbed part of the jet). The full width at half maximum (FWHM) is an indicator of the size of the photosphere of the jet at this frequency. We used this procedure to calculate the frequency–size relationship.

In our model the radio flares are caused by a perturbation in  $\dot{M}$  at the jet-base, leading to a transient density enhancement. This density enhancement during a flare of duration  $t_d$  is quantified by the parameter  $f_n$  so that the number density at the base ( $n_0$ ) as a function of time is given by

$$n_0(t) = \begin{cases} (1 + f_n) n_0 & (0 \leq t \leq t_d) \\ n_0 & \text{otherwise.} \end{cases} \quad (2)$$

As the overdensity propagates outward along the jet, the additional pressure in the overdense region would cool and expand into the neighboring segments with lower pressure and density. While a full computation of this diffusion (and resultant cooling) would require MHD simulations beyond the scope of the present paper, the effect can still be captured by assuming an additional velocity dependent cooling term in the continuity equa-

tion for the overdense region. Assuming that the overdense region expands longitudinally into the neighboring segments with some fraction of the sound speed, we write this additional cooling term as a function of distance from the black hole ( $z$ ) as  $\dot{\gamma}/\gamma = f_o\beta_s c/z$ . Thus  $f_o\beta_s c$  can be interpreted as the longitudinal speed with which the overdense region expands.

### 3. Modeling the quiescent broadband emission and the radio flares from Sgr A\* on July 17, 2006

We test the model against the simultaneous observations of Sgr A\* in 22 and 43 GHz on 2006 July 17 (Yusef-Zadeh et al. 2008), which has the best simultaneous coverage to date of a flare in both frequencies. Indirect evidence suggests that Sgr A\* is seen under large inclination angle (Markoff et al. 2007; Falcke et al. 2009). For simplicity we therefore assume that the jets are perpendicular to our line-of-sight, even though the model can handle any inclination angle. The free parameters of the model are: temperature ( $T_e$ ) and density ( $n_0$ ) of the thermal leptons at the base, location of the sonic point or the nozzle ( $h_0$ ), radius of the nozzle ( $r_0$ ) and its magnetic field ( $B_0$ ). The flare is parametrized by its start time ( $t_0$ ), duration ( $t_d$ ), density enhancement fraction ( $f_n$ ) and expansion speed of the overdense region ( $f_o$ , as a fraction of the sound speed).

The good agreement of the data with model light curves is shown in Fig. 1. The model parameters are given in Table 1. Note that we only model the flare which peaks around 6.5 hours UT in 43 GHz. The increase in flux in both bands during the end of the observations may be the beginning of another flare as suggested by Yusef-Zadeh et al. (2008), but we do not model this due to lack of full coverage. In Fig. 2 we show model predicted light curves at 0.7, 1.3, 2, 3.6, 6 and 13 cm. From Fig. 1 it is clear that the light curves are asymmetric and even a phenomenological model would require (a) rise time-scale, (b) decay time-scale, and (c) amplitude. In our model also three parameters describe the flare completely, viz.  $t_d$  (which can be roughly associated with the rise time),  $f_o$  (associated with decay time), and  $f_n$  (associated with amplitude). It is thus important that a single set of flare parameters fits two rather disparate light curves at two frequencies. Moreover, the decrease of amplitude is consistent with the decrease in average variability with frequency. A compilation of the rms flux variability of Sgr A\* averaged over many flares by Falcke et al. (2009) from VLA and GBI data (Falcke 1999a; Herrnstein et al. 2004) shows that the rms variability decreases with increasing wavelength. The relative amplitude of this flare at both 43 and 22 GHz is about 0.6 times the long-term rms variability, therefore this flare was not extraordinarily bright or faint, and may be considered as a fairly typical flare from Sgr A\*.

The frequency–size relationship predicted by the model is displayed in Fig. 3, showing reasonable agreement with the data at low frequencies where the jet becomes optically thick. The discrepancy at shorter wavelengths where the spectrum is optically thin is expected given that our model ignores general relativistic effects, and simplifies the physics of jet formation and launching, both of which must play an important role very close to the black hole. For this model, the rate at which matter is fed to both jets is  $\dot{M} = 2n_0m_p c\beta_s\gamma_s\pi r_0^2 = 2.4 \times 10^{-9} M_\odot \text{ yr}^{-1}$ , which is about 2 orders of magnitude lower than the upper limit of  $10^{-7} M_\odot \text{ yr}^{-1}$  suggested by linear polarization observations.

## 4. Discussion

In this paper we have shown that a time-dependent relativistic jet model can explain most of the observational features seen in Sgr A\*. The main conclusions of this work are:

- The model presented here can describe the quiescent broadband SED of Sgr A\*, as well as its long-term radio variability.
- Assuming that the radio flares are caused by a transient density enhancement at the base of the jet, which then propagates outward, the model can also fit the 22 and 43 GHz light curve morphology of the flares seen on 2006 July 17 by Yusef-Zadeh et al. (2008). We predict light curve morphology and delays at longer wavelengths, which can be used to test the model with future observations.
- The model predicted frequency–size relationship also matches quite well with the observed radio data.

The radio emission in our model originates in the self-absorbed, optically thick part of the outflow, where adiabatic losses dominate over radiative cooling. Therefore variability in the radio light curves largely traces the expansion of the jet plasma. Assuming that the flares have the same frequency–size relationship as the quiescent emission, the time delay measurements combined with frequency–size measurements strongly constrain the bulk speed of the jet plasma in this model and rule out subrelativistic expansion speeds. An alternate model used by Yusef-Zadeh et al. (2008) to fit the radio light curves assumes adiabatic, subrelativistic expansion of a spherical blob of plasma, i.e. the classic van der Laan (1966) model. Our modeling, at the very least, shows that the van der Laan model is not unique and in fact the jet model, in contrast to the van der Laan model, not only correctly predicts the light curves and the overall variability amplitudes, but also fits the frequency–size relation without violating any other observational constraints. It must be kept in mind that the jet model does not attempt to explain the NIR or X-ray flares. The NIR/X-ray flares trace particle (re)energization and cooling very close to the black hole, while only marginally affecting the optically thick radio flux (Markoff et al. 2001), and no tight correlation between radio and X-ray flares have been found so far. A full general relativistic MHD model including radiative cooling (see e.g. Fragile & Meier 2009; Mościbrodzka et al. 2009) would be required to model the jet launching region. However the simple model presented here captures the important physics and shows that the jet model explains the radio flaring properties naturally, due to simple adiabatic expansion of overdensities in the outflow (likely linked to variations in the accretion rate). Future coordinated multiwavelength campaigns, especially measurements of time-lags, sizes and positional offset at other wavelengths, will enable a better understanding of the velocity profile of the jet from Sgr A\*.

*Acknowledgements.* We would like to thank Farhad Yusef-Zadeh for providing us the data of the radio light curves, and an anonymous referee for valuable comments.

## References

- Blandford, R. D. & Königl, A. 1979, *ApJ*, 232, 34  
 Blumenthal, G. R. & Gould, R. J. 1970, *ApJ*, 42, 237  
 Bower, G. C., Falcke, H., Herrnstein, R. M., et al. 2004, *Science*, 304, 704  
 Chang, J. S. & Cooper, G. 1907, *Journal of Computational Physics*, 6, 1  
 Chiaberge, M. & Ghisellini, G. 1999, *MNRAS*, 306, 113  
 Crusius, A. & Schlickeiser, R. 1986, *A&A*, 164, L16

**Table 1.** Model parameters for the flare of 2006 July 17. The mass ( $M_{\text{BH}}$ ) and distance were taken from their latest estimates (see e.g. Gillessen et al. 2009; Reid et al. 2009). Inclination of the jet axis to the line of sight was fixed to 90 degrees. The base of the jet is parametrized by radius of the nozzle ( $r_0$ ), location of the sonic point ( $h_0$ ), magnetic field strength ( $B_0$ ), number density ( $n_0$ ) and temperature ( $T_e$ ) of the thermal leptons. The flare is characterized by its start time ( $t_0$ ), duration ( $t_d$ ), density enhancement fraction ( $f_n$ ), expansion speed of the overdense region ( $f_o$ , as a fraction of the sound speed). Parameters marked with an asterisk (\*) were not varied during fitting.

Srl. No.	Parameter	Value	Unit
1	$M_{\text{BH}}^*$	4	$10^6 M_{\odot}$
2	Distance*	8.4	kpc
3	Inclination*	90	degrees
4	$r_0$	7	$R_g$
5	$h_0$	9	$R_g$
6	$B_0$	147	Gauss
7	$n_0$	7	$10^4 \text{ cm}^{-3}$
8	$T_e$	7	$10^{10} \text{ K}$
9	$t_0$	5.90	hours UT
10	$t_d$	1800	seconds
11	$f_n$	0.60	
12	$f_o$	0.12	

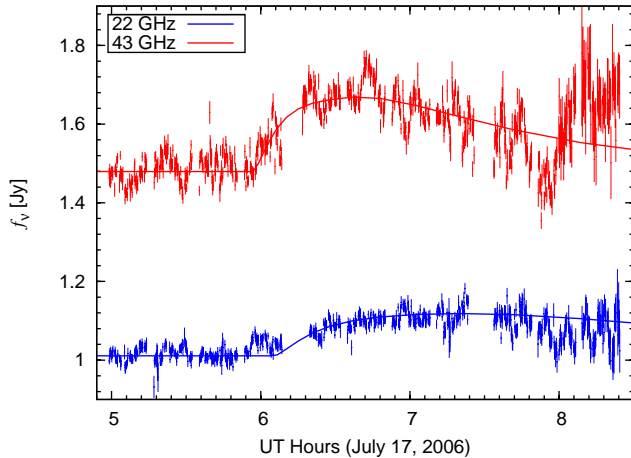


**Fig. 1.** Comparison of model with data for the flare on 2006 July 17 at 43 and 22 GHz. The 43 GHz data with errorbars (from Yusef-Zadeh et al. 2008) are shown in red, and 22 GHz data+model in blue. As noted in §3, we model the flare which created a peak in the 43 GHz light curve near 6.5 hours UT.

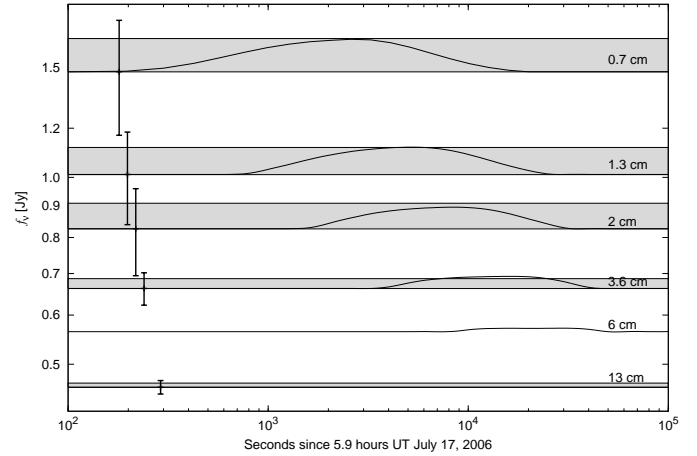


**Fig. 2.** Model predicted light curves of Sgr A\* at key radio frequencies using model parameters shown in Table 1. Also shown as error bars between  $t=200$ – $300$ s are the rms flux variability of Sgr A\* averaged over many flares as compiled by Falcke et al. (2009). The gray bands have a width of 0.6 times the rms variability of Sgr A\*, which is roughly matched to the specific flare under consideration.

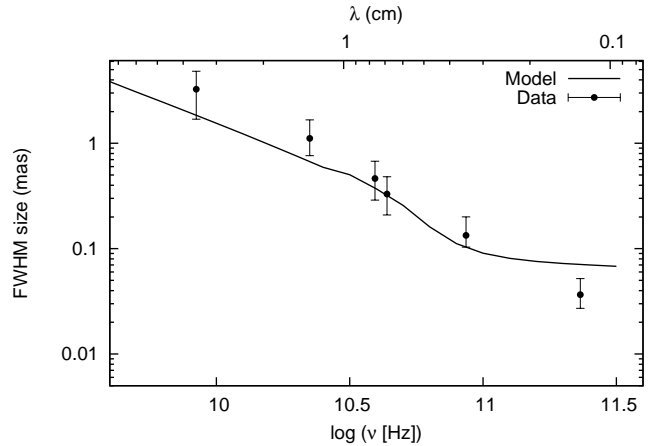


**Fig. 3.** Comparison of model predicted frequency-size relationship (solid line) with observations. The data are from Bower et al. (2004); Shen et al. (2005); Doeleman et al. (2008), which were compiled and corrected for scattering by Falcke et al. (2009).

Dodds-Eden, K., Porquet, D., Trap, G., et al. 2009, *ApJ*, 698, 676  
Doeleman, S., Weintraub, J., Rogers, A. E. E., et al. 2008, *Nature*, 455, 78  
Eckart, A., Schödel, R., García-Marín, M., et al. 2008, *A&A*, 492, 337  
Eckart, A., Baganoff, F. K., Morris, M. R., et al. 2009, *A&A*, 500, 935  
Falcke, H. 1996, *ApJ*, 464, L67  
Falcke, H. 1999a, in *ASP Conf. Ser. 186: The Central Parsecs of the Galaxy*, ed. H. Falcke, A. Cotera, W. Duschl, F. Melia, & M. J. Rieke, 113  
Falcke, H. 1999b, in *ASP Conf. Ser. 186: The Central Parsecs of the Galaxy*, ed. H. Falcke, A. Cotera, W. Duschl, F. Melia, & M. J. Rieke, 148  
Falcke, H. & Biermann, P. L. 1999, *A&A*, 342, 49  
Falcke, H. & Markoff, S. 2000, *A&A*, 362, 113  
Falcke, H., Markoff, S., & Bower, G. C. 2009, *A&A*, 496, 77  
Fragile, P. C. and Meier, D. L. 2009, *ApJ*, 693, 771  
Gallo, E., Fender, R. P., Miller-Jones, J. C. A., et al. 2006, *MNRAS*, 370, 1351  
Genzel, R., Pichon, C., Eckart, A., et al. 2000, *MNRAS*, 317, 348  
Ghez, A. M., Salim, S., Weinberg, N. N., et al. 2008, *ApJ*, 689, 1044  
Gillessen, S., Eisenhauer, F., Trippe, S., et al. 2009, *ApJ*, 692, 1075  
Guilbert, P. W., Fabian, A. C., & Rees, M. J. 1983, *MNRAS*, 205, 593

Herrnstein, R. M., Zhao, J.-H., Bower, G. C., & Goss, W. M. 2004, *AJ*, 127, 3399  
Katarzyński, K., Ghisellini, G., Svensson, R., & Gracia, J. 2006, *A&A*, 451, 739  
de Kool, M., Begelman, M. C. & Sikora, M. 1989, *ApJ*, 337, 66  
Leismann, T., Antón, L., Aloy, M. A., Müller, E., Martí, J. M., Miralles, J. A., & Ibáñez, J. M. 2005, *A&A*, 436, 503  
Leismann, T., Antón, L., Aloy, M. A., et al. 2005, *A&A*, 436, 503  
Lind, K. R. & Blandford, R. D. 1985, *ApJ*, 295, 358  
Liu, S. & Melia, F. 2002, *ApJ*, 566, L77  
Longair, M. S. 1992, *High Energy Astrophysics*, Cambridge University Press.  
Markoff, S. 2005, *ApJ*, 618, L103  
Markoff, S., Falcke, H., Yuan, F., & Biermann, P. L. 2001, *A&A*, 379, L13  
Markoff, S., Bower, G. C., & Falcke, H. 2007, *MNRAS*, 379, 1519  
Marrone, D. P., Baganoff, F. K., Morris, M. R., et al. 2008, *ApJ*, 682, 373  
Marrone, D. P., Moran, J. M., Zhao, J.-H., & Rao, R. 2007, *ApJ*, 654, L57  
Melia, F. 1992, *ApJ*, 387, L25  
Mościbrodzka, M., Gammie, C. F., Dolence, J. C., Shiokawa, H., & Leung, P. K. 2005, *ApJ*, submitted  
Nagar, N. M., Falcke, H., & Wilson, A. S. 2005, *A&A*, 435, 521

- Narayan, R., Mahadevan, R., Grindlay, J. E., Popham, R. G., & Gammie, C. 1998, *ApJ*, 492, 554
- Reid, M. J., Menten, K. M., Zheng, X. W., et al. *ApJ*, 700, 137
- Shen, Z.-Q., Lo, K. Y., Liang, M.-C., Ho, P. T. P., & Zhao, J.-H. 2005, *Nature*, 438, 62
- van der Laan, H. 1966, *Nature*, 211, 1131
- Yuan, F., Shen, Z.-Q., & Huang, L. 2006, *ApJ*, 642, L45
- Yuan, F., Markoff, S., & Falcke, H. 2002, *A&A*, 383, 854
- Yusef-Zadeh, F., Wardle, M., Heinke, C., et al. 2008, *ApJ*, 682, 361
- Yusef-Zadeh, F., Bushouse, H., Wardle, M., et al. 2009, arXiv:0907.3786